Predicting Arsenate Adsorption by Soils using Soil Chemical Parameters in the Constant Capacitance Model

Sabine Goldberg,* S. M. Lesch, D. L. Suarez, and N. T. Basta

ABSTRACT

The constant capacitance model, a chemical surface complexation model, was applied to arsenate, As(V), adsorption on 49 soils selected for variation in soil properties. The constant capacitance model was able to fit arsenate adsorption on all soils by optimizing either three monodentate or two bidentate As(V) surface complexation constants. A general regression model was developed for predicting soil As(V) surface complexation constants from easily measured soil chemical characteristics. These chemical properties were cation exchange capacity (CEC), inorganic C (IOC) content, organic C (OC) content, iron oxide content, and surface area (SA). The prediction equations were used to obtain values for the As(V) surface complexation constants for five additional soils, thereby providing a completely independent evaluation of the ability of the constant capacitance model to describe As(V) adsorption. The model's ability to predict As(V) adsorption was quantitative on three soils, semi-quantitative on one soil, and poor on another soil. Incorporation of these prediction equations into chemical speciation-transport models will allow simulation of soil solution As(V) concentrations under diverse agricultural and environmental conditions without the requirement of soil specific adsorption data and subsequent parameter optimization.

Arsenic is a trace element that is toxic to both plants and animals. Concentrations of As in soils and waters can become elevated as a result of application of arsenical pesticides, disposal of fly ash, mineral dissolution, mine drainage, and geothermal discharge. Elevated concentrations of As are found in agricultural drainage waters from some soils in arid regions. In recognition of the hazards As poses to the welfare of humans and domestic animals, the U.S. Environmental Protection Agency (USEPA) recently lowered the As drinking water standard from 0.667 μmol L^{-1} (50 ppb) to 0.133 μmol L^{-1} (10 ppb) effective 23 Jan. 2006.

Adsorption reactions on soil mineral surfaces can attenuate elevated soil solution As concentrations reducing As contamination to ground waters. Arsenic adsorption is significantly positively correlated with clay and Al and Fe oxide content of soils (Wauchope, 1975; Livesey and Huang, 1981; Yang et al., 2002). Arsenic adsorption studies have been performed on a wide range of adsorbents including oxides, clay minerals, organic matter, carbonates, and whole soils. Arsenic (V) is the thermodynamically stable redox state under oxidizing conditions in soils.

Arsenate adsorption on soils and soil minerals has been described using various modeling approaches. Such models include the empirical distribution coefficient, K_d (de Brouwere et al., 2004), Freundlich and Langmuir isotherm equations (Chakravarty et al., 2002), and surface complexation models: constant capacitance model (Goldberg, 1986, 2002; Goldberg and Glaubig, 1988; Manning and Goldberg, 1996a, 1996b; Goldberg and Johnston, 2001; Gao and Mucci, 2001, 2003), diffuse layer model (Dzombak and Morel, 1990; Hering et al., 1990; Swedlund and Webster, 1999; Lumsdon et al., 2001), triple layer model (Hsia et al., 1992; Khaodhiar et al., 2000; Arai et al., 2004), and CD-MUSIC model (Hiemstra and van Riemsdijk, 1999; Gusstafsson, 2001). Empirical model parameters are only valid for the conditions under which the experiment was conducted. Surface complexation models are chemical models because they define surface species, chemical reactions, mass balances, and charge balance and contain molecular features that can be given thermodynamic significance (Sposito, 1983).

Arsenate has been observed spectroscopically to adsorb specifically on the oxide minerals, goethite, amorphous iron oxide, and amorphous aluminum oxide, forming strong inner-sphere surface complexes containing no water between the adsorbing arsenate ion and the surface functional group (Waychunas et al., 1993; Fendorf et al., 1997; Goldberg and Johnston, 2001). A mixture of monodentate and primarily bidentate arsenate surface complexes was observed on goethite and ferrihydrite (Waychunas et al., 1993).

All surface complexation-modeling approaches indicated above postulated monodentate inner-sphere surface complexes for arsenate adsorption with the exception of the studies of Manning and Goldberg (1996a), Hiemstra and van Riemsdijk (1999), and Gusstaffsson (2001), which considered a combination of mono- and bidentate surface complexes. Arai et al. (2004) found comparable model fits for monodentate and bidentate arsenate surface complexes on hematite. They recommended use of bidentate species to provide closer agreement with the spectroscopic results found on goethite by Waychunas et al. (1993).

Chemical modeling of arsenate adsorption has been performed on natural materials for the clay minerals: kaolinite, montmorillonite, and illite (Manning and Goldberg, 1996b) and a soil (Goldberg and Glaubig, 1988)

S. Goldberg, S.M. Lesch, and D.L. Suarez, USDA-ARS, George E. Brown Jr., Salinity Lab., 450 W. Big Springs Road, Riverside, CA 92507. Contribution from the George E. Brown Jr., Salinity Laboratory. N.T. Basta, School of Natural Resources, Ohio State Univ., 2021 Coffey Road, Columbus, OH 43210-1085. Received 16 Dec. 2004. *Corresponding author (sgoldberg@ussl.ars.usda.gov).

Published in Soil Sci. Soc. Am. J. 69:1389–1398 (2005).
Soil Chemistry
doi:10.2136/sssaj2004.0393

677 S. Segoe Rd., Madison, WI 53711 USA

Abbreviations: ARMSE, average root mean squared error; CEC, cation exchange capacity; Cip, coefficient of imprecision; DF, degrees of freedom; ICP, inductively coupled plasma; IOC, inorganic carbon; MANOCOVA, multivariate analysis of covariance; MSE, mean square error; OC, organic carbon; SA, surface area.

using monodentate surface complexes in the constant capacitance model. Gusstaffsson (2001) evaluated the ability of the CD-MUSIC model to describe arsenate adsorption on a spodic B horizon containing allophane and ferrihydrite by using the monodentate and bidentate arsenate surface complexation constants obtained on gibbsite and ferrihydrite.

The objectives of the present study were: (i) to apply the constant capacitance model to arsenate adsorption on a set of 49 soil samples using both monodentate and bidentate surface configurations for adsorbed arsenate; (ii) to relate arsenate adsorption characteristics and model surface complexation constants to easily measured chemical parameters affecting arsenate adsorption such as surface area (SA), CEC, OC, IOC, aluminum oxide content (Al), and iron oxide content (Fe); (iii) to relate quantitatively variations in these soil properties to variations in values of the arsenate surface complexation constants obtained by the constant capacitance model; and (iv) to evaluate the ability of the constant capacitance model to predict arsenate adsorption on additional soils using the arsenate surface complexation constants calculated from soil chemical properties.

MATERIALS AND METHODS

Arsenate adsorption was investigated using 49 surface and subsurface soil samples from 37 soil series belonging to six different soil orders: 14 mollisols, 10 alfisols, 5 vertisols, 5 entisols, 2 aridisols, and 1 inceptisol. The soils were chosen to provide a wide range of chemical characteristics. Chemical characteristics and soil classifications are provided in Table 1. The subgroup of 21 soil series: Altamont to Yolo constitute a group of soils primarily from California that had been used in prior studies of B (Goldberg et al., 2000) and Mo adsorption (Goldberg et al., 2002). The subgroup of 16 soil series: Bernow to Teller constitute a group of soils from Iowa and Oklahoma that had been used in a prior study of B adsorption (Goldberg et al., 2004).

Soil pH values were measured in deionized water (1:25 soil/water ratio) as described by Thomas (1996). Cation exchange capacities were measured by Na saturation and Mg extraction

Table 1. Classifications and chemical characteristics of soils.

Soil series	Depth	pH	CEC	SA	IOC	OC	Fe	Al
	cm		$mmol_c\ kg^{-1}$	$km^2\ kg^{-1}$	$g\ kg^{-1}$			
Altamont (fine, smectitic, thermic Aridic Haploxerert)	0–25	5.90	152	0.103	0.0099	9.6	7.7	0.58
	25–51	5.65	160	0.114	0.011	6.7	8.2	0.64
Arlington (coarse-loamy, mixed thermic Haplic Durixeralf)	0–25	8.17	107	0.0611	0.30	4.7	8.2	0.48
	25–51	7.80	190	0.103	0.16	2.8	10.1	0.60
Avon (fine, smectitic, mesic, calcic Pachic Argixeroll)	0–15	6.91	183	0.0601	0.083	30.8	4.3	0.78
Bonsall (fine, smectitic, thermic Natric Palexeralf)	0–25	5.88	54	0.0157	0.13	4.9	9.3	0.45
	25–51	5.86	122	0.0329	0.07	2.1	16.8	0.91
Diablo (fine, smectitic, thermic Aridic Haploxerert)	0–15	7.64	301	0.19	0.26	19.8	7.1	1.02
Fallbrook (fine-loamy, mixed, thermic Typic Haploxeralf)	0–25	6.79	112	0.0683	0.023	3.5	6.9	0.36
	25–51	6.35	78	0.0285	0.24	3.1	4.9	0.21
Fiander (fine-silty, mixed, mesic Typic Natraquoll)	0–15	9.60	248	0.0925	6.9	4.0	9.2	1.06
Haines (coarse-silty, mixed, superactive, calcareous, mesic Typic Endoaquept)	20	9.05	80	0.0595	15.8	14.9	1.7	0.18
Hanford (coarse-loamy, mixed, superactive nonacid, thermic Typic Xerorthent)	0–10	8.40	111	0.0289	10.1	28.7	6.6	0.35
Holtville (clayey over loamy, smectitic over mixed, superactive, calcareous, hyperthermic Typic Torrifluvent)	61–76	8.93	58	0.043	16.4	2.1	4.9	0.27
Imperial (fine, smectitic, calcareous, hyperthermic Vertic Torrifluvent)	15–46	8.58	198	0.106	17.9	4.5	7.0	0.53
Nohili (very-fine, smectitic, calcareous, isohyperthermic Cumulic Endoaquoll)	0–23	8.03	467	0.286	2.7	21.3	49.0	3.7
Pachappa (coarse-loamy, mixed, thermic Mollic Haploxeralf)	0–25	6.78	39	0.0151	0.026	3.8	7.6	0.67
	25–51	7.02	52	0.041	0.014	1.1	7.2	0.35
Porterville (fine, smectitic, thermic Aridic Haploxerert)	0–7.6	6.83	203	0.137	0.039	9.4	10.7	0.90
Ramona (fine-loamy, mixed, superactive, thermic Typic Haploxeralf)	0–25	5.89	66	0.0279	0.02	4.4	4.5	0.42
	25–51	6.33	29	0.0388	0.018	2.2	5.9	0.40
Reagan (fine-silty, mixed, superactive, thermic Ustic Haplocalcid)	Surface	8.39	98	0.0588	18.3	10.1	4.6	0.45
Ryepatch (very-fine, smectitic, calcareous, mesic Fluvaquentic Vertic Endoaquoll)	0–15	7.98	385	0.213	2.5	32.4	2.6	0.92
Sebree (fine-silty, mixed, superactive, mesic Xeric Natridurid)	0–13	5.99	27	0.0212	0.0063	2.2	6.0	0.46
Wasco (coarse-loamy, mixed, superactive, nonacid, thermic Typic Torriorthent)	0–5.1	5.01	71	0.0309	0.009	4.7	2.4	0.42
Wyo (fine-loamy, mixed, superactive thermic Mollic Haploxeralf)		6.26	155	0.0539	0.014	19.9	9.5	0.89
Yolo (fine-silty, mixed, superactive, nonacid, thermic Mollic Xerofluvent)	0–15	8.43	177	0.0730	0.23	11.5	15.6	1.13
Bernow (fine-loamy, siliceous, active, thermic Glossic Paleudalf)	B	4.15	77.6	0.0464	0.0028	3.8	8.1	1.1
Canisteo (fine-loamy, mixed, superactive, calcareous, mesic Typic Endoaquoll)	A	8.06	195	0.152	14.8	34.3	1.7	0.44
Dennis (fine, mixed, active thermic Aquic Argiudoll)	A	5.27	85.5	0.0403	0.0014	18.6	12.9	1.7
	B	5.43	63.1	0.0724	0.0010	5.2	30.0	4.1
Dougherty (loamy, mixed, active, thermic Arenic Haplustalf)	A	4.98	3.67	0.241	0.0010	7.0	1.7	0.28
Hanlon (coarse-loamy, mixed, superactive, mesic Cumulic Hapludoll)	A	7.41	142	0.0587	2.6	15.1	3.7	0.45
Kirkland (fine, mixed, superactive, thermic Udertic Paleustoll)	A	5.05	154	0.0421	0.014	12.3	5.6	0.80
Luton (fine, smectitic, mesic Typic Endoaquert)	A	6.92	317	0.169	0.099	21.1	9.1	0.99
Mansic (fine-loamy, mixed, superactive, thermic Aridic Calciustoll)	A	8.32	142	0.0422	16.7	10.1	2.7	0.40
	B	8.58	88.1	0.0355	63.4	9.0	1.1	0.23
Norge (fine-silty, mixed, active, thermic Udic Paleustoll)	A	3.86	62.1	0.0219	0.0010	11.6	6.1	0.75
Osage (fine, smectitic, thermic Typic Epiaquert)	A	6.84	377	0.134	0.59	29.2	15.9	1.4
	B	6.24	384	0.143	0.0100	18.9	16.5	1.3
Pond Creek (fine-silty, mixed, superactive, thermic Pachic Argiustoll)	A	4.94	141	0.0354	0.0023	16.6	5.2	0.70
	B	6.78	106	0.0596	0.016	5.0	5.1	0.81
Pratt (sandy, mixed, mesic Lamellic Haplustalf)	A	5.94	23.9	0.0123	0.0026	4.2	1.2	0.18
	B	5.66	23.3	0.117	0.0007	2.1	0.92	0.13
Richfield (fine, smectitic, mesic Aridic Argiustoll)	B	7.12	275	0.082	0.040	8.0	5.4	0.76
Summit (fine, smectitic, thermic Oxyaquic Vertic Argiudoll)	A	7.03	374	0.218	0.25	26.7	16.2	2.3
	B	6.23	384	0.169	0.0079	10.3	17.8	2.5
Taloka (fine, mixed, active, thermic Mollic Albaqualf)	A	4.88	47.4	0.087	0.0021	9.3	3.6	0.62
Teller (fine-loamy, mixed, active, thermic Udic Argiustoll)	A	4.02	43.1	0.227	0.0008	6.8	3.2	0.53

as described by Rhoades (1982) for arid-zone soils. Surface areas were determined using ethylene glycol monoethyl ether (EGME) adsorption (Cihacek and Bremner, 1979). Free Fe and Al were extracted with a Na citrate/citric acid buffer and Na hydrosulphite as described by Coffin (1963) and measured using inductively coupled plasma (ICP) emission spectrometry. Carbon contents were determined using a UIC Full Carbon System 150 with a C coulometer[1] (UIC, Inc., Joliet, IL). Organic C was calculated as the difference between total C determined by furnace combustion at 950°C and IOC determined using an acidification module and heating. The soil samples represented a broad range of chemical characteristics: pH: 3.9 to 9.6, CEC: 3.7 to 384 $mmol_c\ kg^{-1}$, SA: 0.0123 to 0.286 $km^2\ kg^{-1}$, IOC: 0.0007 to 63 $g\ kg^{-1}$, OC: 1.1 to 34 $g\ kg^{-1}$, free Fe oxide: 0.9 to 49 $g\ kg^{-1}$, free Al oxide: 0.13 to 4.1 $g\ kg^{-1}$.

Arsenate adsorption experiments were performed in batch systems to determine adsorption envelopes [amount of As(V) adsorbed as a function of solution pH at fixed total As(V) mass]. One gram of soil was added to 50-mL polypropylene centrifuge tubes and equilibrated with 25 mL of a 0.1 *M* NaCl solution by shaking for 2 h on a reciprocating shaker. This reaction time had been used in a prior study of arsenate adsorption by soil (Goldberg and Glaubig, 1988). The equilibrating solution contained 20 $\mu mol\ L^{-1}$ As(V) and had been adjusted to the desired pH range of 3 to 10 using 1 *M* HCl or 1 *M* NaOH. These acid or base additions changed the total volumes by <2%. After reaction, the samples were centrifuged and the decantates analyzed for pH, passed through 0.45-μm membrane filters, and analyzed for As concentration using ICP spectrometry. Initial analyses using the direct speciation method of Manning and Martens (1997) verified that no reduction of As(V) to As(III) had occurred.

A detailed discussion of the theory and assumptions of the constant capacitance surface complexation model is provided in Goldberg (1992). In the present application of the model to arsenate adsorption, the following surface complexation constants were considered:

$$SOH_{(s)} + H^+_{(aq)} \rightleftharpoons SOH^+_{2(s)} \quad [1]$$

$$SOH_{(s)} \rightleftharpoons SO^-_{(s)} + H^+_{(aq)} \quad [2]$$

$$SOH_{(s)} + H_3AsO_{4(aq)} \rightleftharpoons SH_2AsO_{4(s)} + H_2O \quad [3]$$

$$SOH_{(s)} + H_3AsO_{4(aq)} \rightleftharpoons SHAsO^-_{4(s)} + H^+_{(aq)} + H_2O \quad [4]$$

$$SOH_{(s)} + H_3AsO_{4(aq)} \rightleftharpoons SAsO^{2-}_{4(s)} + 2H^+_{(aq)} + H_2O \quad [5]$$

$$2SOH_{(s)} + H_3AsO_{4(aq)} \rightleftharpoons S_2HAsO_{4(s)} + 2H_2O \quad [6]$$

$$2SOH_{(s)} + H_3AsO_{4(aq)} \rightleftharpoons S_2AsO^-_{4(s)} + H^+_{(aq)} + 2H_2O \quad [7]$$

where $SOH_{(s)}$ represents reactive surface hydroxyl groups on oxides and aluminol groups on clay minerals in the soils. By convention, surface complexation reactions in the constant capacitance model are written starting with the completely undissociated acids; however, the model application contains the aqueous speciation reactions for As(V). Both monodentate and bidentate arsenate surface species were considered, consistent with spectroscopic observations.

Intrinsic equilibrium constants for the surface complexation reactions are:

$$K_+\ (\text{int}) = \frac{[SOH^+_2]}{[SOH][H^+]} \exp(F\psi/RT) \quad [8]$$

$$K_-\ (\text{int}) = \frac{[SO^-][H^+]}{[SOH]} \exp(-F\psi/RT) \quad [9]$$

$$K^1_{As}(\text{int}) = \frac{[SH_2AsO_4]}{[SOH][H_3AsO_4]} \quad [10]$$

$$K^2_{As}(\text{int}) = \frac{[SHAsO^-_4][H^+]}{[SOH][H_3AsO_4]} \exp(-F\psi/RT) \quad [11]$$

$$K^3_{As}(\text{int}) = \frac{[SAsO^{2-}_4][H^+]^2}{[SOH][H_3AsO_4]} \exp(-2F\psi/RT) \quad [12]$$

$$K^4_{As}(\text{int}) = \frac{[S_2HAsO_4]}{[SOH]^2[H_3AsO_4]} \quad [13]$$

$$K^5_{As}(\text{int}) = \frac{[S_2AsO^-_4][H^+]}{[SOH]^2[H_3AsO_4]} \exp(-F\psi/RT) \quad [14]$$

where F is the Faraday constant ($C\ mol_c^{-1}$), ψ is the surface potential (V), R is the molar gas constant ($J\ mol^{-1}\ K^{-1}$), T is the absolute temperature (K), and square brackets indicate concentrations ($mol\ L^{-1}$). The bidentate surface complexation constants are dependent on the concentration of [SOH] because the [SOH] term is squared. The assumption is made that the number of bidentate sites, $\equiv S_2$, is equal to one half of the monodentate sites, $\equiv S$. The number of bidentate sites available for adsorption is actually less than that because the two monodentate sites used to form the bidentate surface complex must be adjacent to each other (Benjamin, 2002). The exponential terms can be considered as solid-phase activity coefficients correcting for charge on the charged surface complexes.

Mass balance of the surface functional groups for monodentate adsorption is:

$$[SOH]_T = [SOH] + [SOH^+_2] + [SO^-] + [SH_2AsO_4] + [SHAsO^-_4] + [SAsO^{2-}_4] \quad [15]$$

and mass balance for bidentate adsorption is:

$$[SOH]_T = [SOH] + [SOH^+_2] + [SO^-] + 2[S_2HAsO_4] + 2[S_2AsO^-_4] \quad [16]$$

Charge balance for monodentate adsorption is:

$$\sigma = [SOH^+_2] - [SO^-] - [SHAsO^-_4] - 2[SAsO^{2-}_4] \quad [17]$$

and charge balance for bidentate adsorption is:

$$\sigma = [SOH^+_2] - [SO^-] - [S_2AsO^-_4] \quad [18]$$

where σ has units of ($mol_c\ L^{-1}$).

The computer program FITEQL 3.2 (Herbelin and Westall, 1996) was used to fit arsenate surface complexation constants to the experimental adsorption data. The program uses a nonlinear least squares optimization routine to fit equilibrium constants to experimental data and contains the constant capacitance model of adsorption. FITEQL can also be used to predict chemical speciation using previously determined equilibrium constant values. In the present application, surface complexation constants for monodentate and bidentate arsenate species were determined in separate optimizations. The assumption that arsenate adsorption takes place on one set of reactive surface functional groups is clearly a gross simplification since soils are complex multisite mixtures containing a variety of surface sites. Soil surface complexation constants are average composite values that include competing ion effects and soil mineralogical characteristics.

Input parameter values for the model were: SA, capacitance: $C = 1.06\ F\ m^{-2}$ (considered optimum for Al oxide by

[1] Trade names and company names are included for the benefit of the reader and do not imply any endorsement or preferential treatment of the product listed by the U.S. Department of Agriculture.

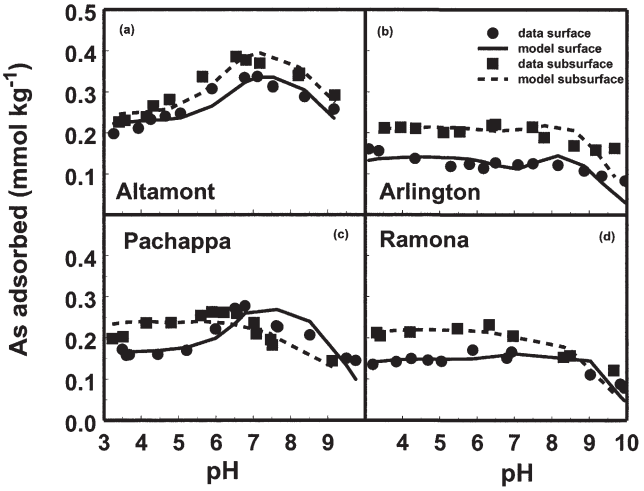

Fig. 1. Fit of the constant capacitance model to As(V) adsorption on Southwestern soils: (a) Altamont soil; (b) Arlington soil; (c) Pachappa soil; and (d) Ramona soil. Experimental data are represented by circles for the surface 0 to 25 cm and by squares for the subsurface 25 to 51 cm. Model fits are represented by solid lines for the surface and dashed lines for the subsurface.

Westall and Hohl, 1980), protonation constant: $\log K_{+}(\text{int}) = 7.35$, dissociation constant: $\log K_{-}(\text{int}) = -8.95$ (averages of a literature compilation for Al and Fe oxides from Goldberg and Sposito, 1984), and total number of reactive surface hydroxyl groups: $[\text{SOH}]_T = 21$ μmol L^{-1}. Previous sensitivity analyses showed that more than tripling the capacitance produced only minor changes in the values of the surface complexation constants (Goldberg and Sposito, 1984) and that surface complexation was highly dependent on surface site density (Goldberg, 1991). Constant values of capacitance and surface site density are necessary to allow application of model results to predicting adsorption by additional soils. Goodness-of-fit was evaluated using the overall variance V in Y:

$$V_Y = \text{SOS/DF} \qquad [19]$$

where SOS is the weighted sum of squares of the residuals and DF is the degrees of freedom.

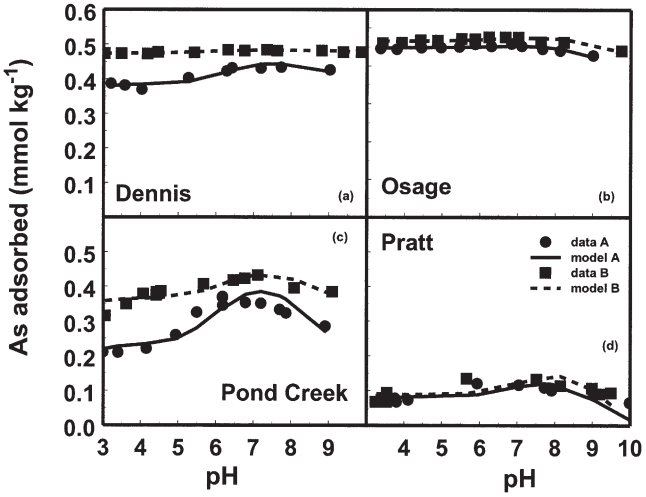

Fig. 2. Fit of the constant capacitance model to As(V) adsorption by Midwestern soils: (a) Dennis soil; (b) Osage soil; (c) Pond Creek soil; and (d) Pratt soil. Experimental data are represented by circles for the A horizon and by squares for the B horizon. Model fits are represented by solid lines for the A horizon and dashed lines for the B horizon.

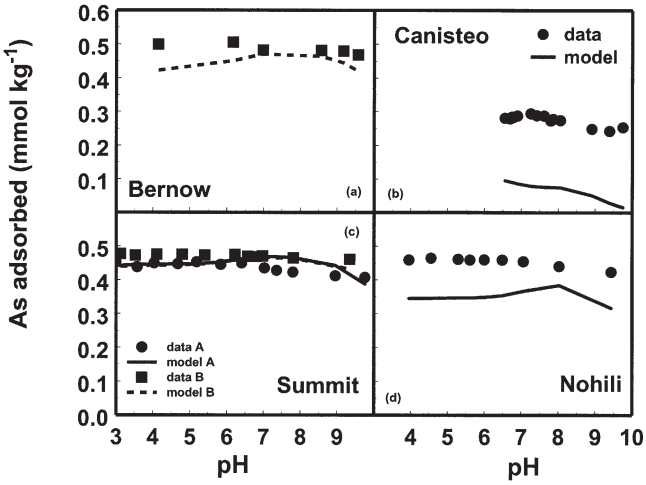

Fig. 3. Prediction of As(V) adsorption with the constant capacitance model on soils not used to obtain the prediction equations: (a) Bernow soil; (b) Canisteo soil; (c) Summit soil; and (d) Nohili soil. Experimental data are represented by circles for the surface 0 to 25 cm and A horizons and by squares for the B horizon. Model predictions are represented by solid lines for the surface 0 to 25 cm and A horizons and dashed lines for the B horizon.

RESULTS AND DISCUSSION

Arsenate adsorption as a function of solution pH was determined for 49 different soil samples (examples are presented in Fig. 1 to 3). Arsenate adsorption generally increased with increasing solution pH, exhibited a maximum in adsorption around pH 6 to 7, and decreased with further increases in solution pH.

The constant capacitance model was fit to the As(V) adsorption envelopes of all the soil samples. Surface complexation constants for both monodentate and bidentate surface configurations of adsorbed As(V) were optimized in separate calculations. Model fits were superior in quality (as measured by the goodness-of-fit criterion, V_Y) when monodentate As(V) surface species were used. The model optimization was able to fit the three monodentate surface complexation constants, $\log K^1_{As}(\text{int})$, $\log K^2_{As}(\text{int})$, and $\log K^3_{As}(\text{int})$, simultaneously for all soils except Bernow, Canisteo, Summit A, Summit B, and Nohili where only two constants were optimized since the $\log K^2_{As}(\text{int})$ constant did not converge. Table 2 provides values for the optimized surface complexation constants. Simultaneous optimization is considered necessary for developing prediction equations because of the high degree of correlation of the three As(V) surface complexation constants. For this reason, the Bernow, Canisteo, Summit A, Summit B, and Nohili soils were not included in the regression model database.

Figures 1 and 2 indicate the ability of the constant capacitance model to describe As(V) adsorption on 16 soils by simultaneously optimizing $\log K^1_{As}(\text{int})$, $\log K^2_{As}(\text{int})$, and $\log K^3_{As}(\text{int})$. In almost all cases, the model provided a quantitative description of the adsorption data. The subset of soils chosen for presentation in these figures were soils for which we were able to determine As(V) adsorption envelopes on both surface and subsurface horizons. The range in quality of model fits is well representative of the entire set of soils studied. For each soil, the model

Table 2. Constant capacitance model surface complexation constants.

Soil series	Depth	Fitted $LogK^1_{As}$	Fitted $LogK^2_{As}$	Fitted $LogK^3_{As}$	Predicted $LogK^1_{As}$	Predicted $LogK^2_{As}$	Predicted $LogK^3_{As}$	Jack-knife predicted $LogK^1_{As}$	Jack-knife predicted $LogK^2_{As}$	Jack-knife predicted $LogK^3_{As}$	Average absolute error
	cm										
Altamont	0–25	9.99	3.92	−3.89	9.88	3.56	−4.10	9.86	3.51	−4.13	0.26
	25–51	10.09	4.41	−3.69	9.98	3.56	−4.08	9.96	3.45	−4.13	0.51
Arlington	0–25	9.57	2.04	−4.59	9.99	3.20	−4.15	10.01	3.27	−4.12	0.71
	25–51	9.95	2.92	−4.24	10.20	3.33	−4.10	10.24	3.40	−4.08	0.31
Avon	0–15	9.29	3.02	−4.52	9.38	3.22	−4.42	9.40	3.28	−4.39	0.17
Bonsall	0–25	9.50	2.77	−4.64	9.92	3.20	−4.15	9.98	3.25	−4.09	0.50
	25–51	10.90	3.64	−3.27	10.47	3.56	−3.82	10.35	3.53	−3.98	0.46
Diablo	0–15	9.26	3.14	−4.45	9.90	3.51	−3.96	10.03	3.58	−3.86	0.60
Fallbrook	0–25	10.02	3.00	−4.20	9.93	3.30	−4.27	9.92	3.32	−4.27	0.17
	25–51	9.56	2.84	−4.62	9.68	2.85	−4.57	9.70	2.85	−4.56	0.07
Fiander	0–15	10.08	2.10	−4.76	10.14	3.06	−4.14	10.15	3.30	−3.98	0.69
Haines	20	9.43	2.39	−4.01	9.33	2.60	−4.45	9.28	2.69	−4.64	0.63
Hanford	0–10	9.83	3.04	−4.16	9.53	2.92	−4.28	9.38	2.86	−4.34	0.27
Holtville	61–76	10.32	3.66	−3.88	9.97	2.67	−4.26	9.85	2.35	−4.38	0.76
Imperial	15–46	10.23	3.77	−3.77	10.10	2.98	−4.08	10.06	2.78	−4.16	0.52
Nohili	0–23	12.82		−2.21	10.74	4.04	−3.17				1.52
Pachappa	0–25	9.67	3.55	−4.15	9.91	3.26	−4.15	9.94	3.22	−4.15	0.20
	25–51	10.03	3.06	−4.44	10.05	3.16	−4.33	10.05	3.18	−4.30	0.09
Porterville	0–7.6	10.36	3.89	−3.60	10.14	3.68	−3.84	10.10	3.64	−3.89	0.26
Ramona	0–25	9.58	2.79	−4.37	9.55	3.02	−4.59	9.55	3.06	−4.63	0.19
	25–51	9.96	2.99	−4.46	9.93	3.19	−4.18	9.92	3.22	−4.14	0.19
Reagan	Surface	9.66	2.94	−4.07	9.74	2.84	−4.18	9.76	2.83	−4.20	0.11
Ryepatch	0–15	9.40	3.07	−4.70	9.50	3.11	−4.26	9.54	3.13	−4.06	0.28
Sebree	0–13	9.64	3.28	−4.70	9.76	3.11	−4.41	9.80	3.07	−4.33	0.24
Wasco	0–5.1	9.65	3.31	−4.45	9.46	3.04	−4.59	9.39	2.95	−4.64	0.27
Wyo		10.36	3.67	−3.80	9.79	3.62	−4.06	9.66	3.60	−4.12	0.36
Yolo	0–15	10.00	3.96	−3.86	10.09	3.51	−3.93	10.11	3.42	−3.94	0.24
Bernow	B	12.84		−1.78	11.21	5.29	−2.40				1.12
Canisteo	A	10.54		−3.70	9.39	2.21	−5.11				1.27
Dennis	A	10.99	5.02	−2.57	11.06	5.28	−2.77	11.08	5.34	−2.82	0.22
	B	12.51	6.93	−0.73	12.50	6.97	−0.83	12.48	7.12	−1.16	0.22
Dougherty	A	9.49	3.23	−4.21	9.69	3.21	−4.13	10.14	3.16	−3.95	0.32
Hanlon	A	10.11	3.18	−4.17	10.35	3.61	−3.66	10.40	3.71	−3.55	0.48
Kirkland	A	10.44	5.25	−3.14	10.42	4.26	−3.60	10.42	4.14	−3.65	0.55
Luton	A	10.46	4.46	−3.31	10.96	4.66	−3.23	11.10	4.72	−3.20	0.33
Mansic	A	9.71	3.05	−4.24	10.26	3.34	−3.65	10.50	3.45	−3.41	0.67
	B	10.21	2.58	−3.65	9.47	2.19	−4.53	8.86	1.88	−5.26	1.22
Norge	A	10.31	3.90	−3.99	10.37	4.46	−3.47	10.38	4.61	−3.34	0.48
Osage	A	11.75	5.08	−2.63	11.55	5.27	−2.49	11.47	5.34	−2.43	0.25
	B	12.26	5.97	−1.86	11.43	5.50	−2.66	11.19	5.36	−2.90	0.91
Pond Creek	A	10.02	4.44	−3.86	10.09	4.04	−4.05	10.11	3.91	−4.11	0.29
	B	10.85	4.98	−3.01	10.73	4.53	−3.09	10.71	4.44	−3.10	0.26
Pratt	A	9.14	2.56	−4.78	9.09	2.73	−4.75	9.06	2.85	−4.72	0.14
	B	9.26	2.55	−4.64	9.17	2.69	−4.87	9.12	2.77	−5.01	0.24
Richfield	B	10.00	3.85	−4.17	10.62	4.34	−3.45	10.73	4.42	−3.33	0.71
Summit	A	11.65		−2.57	11.58	5.34	−2.51				0.07
	B	13.14		−1.61	11.73	5.85	−2.24				1.02
Taloka	A	10.25	4.11	−3.89	10.09	3.88	−3.92	10.07	3.85	−3.92	0.16
Teller	A	10.20	3.61	−4.34	10.10	3.87	−3.99	10.08	3.95	−3.89	0.31

fit is comparable in quality for both horizons. The quality of fit for the Southwestern soils, Fig. 1, is comparable with that for the Midwestern soils, Fig. 2.

A general regression modeling approach was used to relate the As(V) surface complexation constants to the following set of soil chemical properties: CEC, SA, IOC, OC, Fe, and Al. The 44 soils used to obtain the regression model results discussed below had the following ranges of soil properties: CEC, 3.7 to 385 $mmol_c\ kg^{-1}$; SA, 0.0123 to 0.241 $km^2\ kg^{-1}$; IOC, 0.0007 to 63.4 $g\ kg^{-1}$; OC, 1.1 to 34.3 $g\ kg^{-1}$; Fe, 1.1 to 30 $g\ kg^{-1}$; and Al, 0.13 to 2.5 $g\ kg^{-1}$. The following initial regression model was specified for each of the surface complexation constants:

$$\log K_j = \beta_{0j} + \beta_{1j}(\ln CEC) + \beta_{2j}(\ln SA) + \beta_{3j}(\ln IOC) + \beta_{4j}(\ln OC) + \beta_{5j}(\ln Fe) + \beta_{6j}(\ln Al) + \varepsilon \quad [20]$$

where the β_{ij} parameters represent the empirically derived regression coefficients (associated with the log transformed soil properties) and ε represents the residual error component. An initial analysis of this model yielded rather poor results [R^2 values of 0.494, 0.592, and 0.462 for $logK^1_{As}(int)$, $logK^2_{As}(int)$, and $logK^3_{As}(int)$, respectively]. Additionally, none of the soil properties appeared to display any substantial predictive potential. However, the 44 soils considered in this analysis came from two distinct populations (18 Midwestern soils and 26 Southwestern soils). A Hotelling's T^2 test (Johnson and Wichern, 1988) confirmed that the mean surface complexation constant values were statistically different between these two groups ($F = 3.82$, $p = 0.017$) and an additional statistical analysis suggested that these two populations exhibited different soil property/adsorption constant relationships.

For this reason, Eq. [20] was respecified as a multivariate analysis of covariance (MANOCOVA) model so that distinct regression model parameters could be si-

Table 3. Regression model identification: Summary prediction statistics for each step.

Step	Action	Constant	Adjusted R^2	Jack-knife MSE‡
0	Full MANOCOVA model	$LogK^1_{As}$	0.736	0.240
		$LogK^2_{As}$	0.732	0.366
		$LogK^3_{As}$	0.716	0.317
1	(a) common intercepts imposed across groups, (b) ln(Al) parameters removed	$LogK^1_{As}$	0.754	0.192
		$LogK^2_{As}$	0.737	0.310
		$LogK^3_{As}$	0.719	0.264
2	(a) common ln(CEC) parameters imposed across groups	$LogK^1_{As}$	0.761	0.181
		$LogK^2_{As}$	0.744	0.297
		$LogK^3_{As}$	0.728	0.250
3	(a) common ln(IOC) parameters imposed across groups	$LogK^1_{As}$	0.756†	0.175
		$LogK^2_{As}$	0.744	0.287
		$LogK^3_{As}$	0.709†	0.264†

† Degraded adjusted R^2 or jack-knife MSE estimate.
‡ MSE, mean squared error.

multaneously estimated for each population (Johnson and Wichern, 1988). This MANOCOVA model was then used to test for (i) the overall statistical significance of each predictive soil property, and (ii) statistically equivalent parameter estimates across populations. Since the purpose of this MANOCOVA model is primarily prediction (rather than inference), two criteria were used in determining the final form of the equation: classical multivariate hypothesis testing and jack-knifed mean square error estimates (as computed from the jack-knifed PRESS residuals [Myers (1986)]. Specifically, a particular soil property was removed from the model if, and only if, its removal was: (i) clearly justified by the multivariate Wilks lambda significance test ($p > 0.15$); and (ii) the jack-knifed mean square error, MSE, estimates associated with all three surface complexation constants decreased after removing the regression parameters (associated with this soil property). Likewise, group-specific regression parameters (for a specific soil property) were only deemed to be equivalent if again such equivalence was: (i) clearly justified by the significance test ($p > 0.15$); and (ii) the resulting jack-knifed MSE estimates improved in all three equations.

Some pertinent summary prediction statistics for the full MANOCOVA models are shown in the top part of Table 3 (Step 0 statistics). Recall that these full MANOCOVA models essentially represent Eq. [20] individually fit to each soil group (but with the residuals pooled across groups). The jack-knifed MSE estimates for these three surface complexation model prediction equations were 0.240, 0.366, and 0.317 for the $logK^1_{As}$(int), $logK^2_{As}$(int), and $logK^3_{As}$(int), respectively.

The first round of multivariate significance tests clearly indicated that a common intercept assumption was reasonable for all three surface complexation constant equations ($F = 0.18$, $p = 0.909$), and that the ln(Al) regression parameter could be removed completely from each equation ($F = 0.86$, $p = 0.529$). Hence, the common intercept restriction was imposed, the ln(Al) parameter was dropped from each model in Step 1, and new jack-knifed MSE estimates were calculated. As shown in Table 3, these jack-knifed MSE estimates associated with each surface complexation constant equation improved (i.e., became smaller). A second round of multivariate significance tests was performed. These new tests indicated that a common ln(CEC) assumption was reasonable in each surface complexation constant equation ($F = 0.05$, $p = 0.984$). After imposing this additional restriction, the revised jack-knifed MSE estimates again improved across all three equations (to 0.181, 0.297, and 0.250, respectively).

A third round of multivariate significance tests was then performed. All of the remaining parameter removal tests were statistically significant at or below the α 0.1 level. Likewise, all but one of the parameter equivalence tests were statistically significant at or below the α 0.05 level. The one nonsignificant test result was the common ln(IOC) test ($F = 1.14$, $p = 0.349$). However, on imposing this new equivalence constraint, the jack-knifed MSE estimate associated with the $logK^3_{As}$(int) equation increased (from 0.250 to 0.264). Although the adjusted R^2 values were not considered in the formal model identification process, Table 3 shows that two of these adjusted R^2 values were also degraded after imposing the common ln(IOC) constraint. Therefore, since all other test results were statistically significant and the common ln(IOC) constraint was found to degrade the jack-knifed prediction accuracy [in the $logK^3_{As}$(int) equation], the set of Step 2 equations was selected as the optimal set of surface complexation constant prediction equations.

The final model summary statistics, standard errors, and parameter estimates for each surface complexation constant regression equation are shown in Table 4. The final individual significance tests are also shown by soil grouping. Note that the intercept and ln(CEC) parameters are identical across groups, since these parameters were constrained to be equivalent (across groups) in the MANOCOVA models.

A full set of residual analyses was performed after identifying these final equations. All three residual distributions were devoid of any outliers and passed the Shapiro-Wilk test for Normality. Additionally, the assumption of equivalent multivariate residual distributions across soil groups was not rejected by an asymptotic Chi-squared test ($\chi^2 = 7.09$, $p = 0.313$), suggesting that the MANOCOVA modeling assumptions were satisfied.

A "jack-knifing" procedure was performed on each surface complexation constant regression equation to assess its predictive ability. Jack-knifing is a technique where each observation is sequentially set aside, the model is reestimated without the use of this observation, and the set-aside observation is then predicted from the

Table 4. Regression model summary statistics, parameter estimates, and standard errors.

Model summary statistics					
Constant	**R^2**	**Adjusted R^2**	**MSE**	**Model *F*-score**	**Prob. > *F***
$LogK^1_{As}$	**0.811**	**0.761**	**0.124**	**16.24**	**<0.0001**
$LogK^2_{As}$	**0.798**	**0.744**	**0.259**	**14.91**	**<0.0001**
$LogK^3_{As}$	**0.785**	**0.728**	**0.175**	**13.76**	**<0.0001**
Parameter estimates					
Constant	**Parameter**	**Parameter estimate**	**Parameter standard error**	***t*-score**	**Prob. > |*t*|**
$LogK^1_{As}$	**intercept**	**10.639**	**0.604**	**17.62**	**<0.0001**
	ln(CEC)	**−0.107**	**0.107**	**−1.00**	**0.322**
Group 1†	**ln(IOC)**	**0.078**	**0.034**	**2.31**	**0.027**
Group 1	**ln(OC)**	**−0.365**	**0.166**	**−2.21**	**0.034**
Group 1	**ln(Fe)**	**1.087**	**0.143**	**7.60**	**<0.0001**
Group 1	**ln(SA)**	**0.094**	**0.098**	**0.96**	**0.344**
Group 2‡	**ln(IOC)**	**0.022**	**0.028**	**0.80**	**0.428**
Group 2	**ln(OC)**	**−0.143**	**0.088**	**−1.63**	**0.113**
Group 2	**ln(Fe)**	**0.385**	**0.137**	**2.82**	**0.008**
Group 2	**ln(SA)**	**0.256**	**0.111**	**2.31**	**0.027**
$LogK^2_{As}$	**intercept**	**3.385**	**0.873**	**3.88**	**0.001**
	ln(CEC)	**−0.083**	**0.154**	**−0.54**	**0.595**
Group 1	**ln(IOC)**	**−0.002**	**0.049**	**−0.04**	**0.968**
Group 1	**ln(OC)**	**−0.400**	**0.239**	**−1.67**	**0.104**
Group 1	**ln(Fe)**	**1.360**	**0.207**	**6.58**	**<0.0001**
Group 1	**ln(SA)**	**0.018**	**0.142**	**0.13**	**0.898**
Group 2	**ln(IOC)**	**−0.061**	**0.040**	**−1.54**	**0.132**
Group 2	**ln(OC)**	**0.104**	**0.127**	**0.82**	**0.419**
Group 2	**ln(Fe)**	**0.313**	**0.198**	**1.58**	**0.123**
Group 2	**ln(SA)**	**0.247**	**0.160**	**1.54**	**0.133**
$LogK^3_{As}$	**intercept**	**−2.579**	**0.716**	**−3.60**	**0.001**
	ln(CEC)	**−0.296**	**0.127**	**−2.34**	**0.025**
Group 1	**ln(IOC)**	**0.115**	**0.040**	**2.86**	**0.007**
Group 1	**ln(OC)**	**−0.570**	**0.196**	**−2.91**	**0.006**
Group 1	**ln(Fe)**	**1.382**	**0.170**	**8.15**	**<0.0001**
Group 1	**ln(SA)**	**−0.004**	**0.117**	**−0.04**	**0.970**
Group 2	**ln(IOC)**	**0.024**	**0.033**	**0.74**	**0.467**
Group 2	**ln(OC)**	**0.085**	**0.104**	**0.82**	**0.420**
Group 2	**ln(Fe)**	**0.363**	**0.162**	**2.23**	**0.032**
Group 2	**ln(SA)**	**0.376**	**0.132**	**2.85**	**0.007**

† Midwestern soils.
‡ Southwestern soils.

remaining data. The final set of 44 jack-knife predicted As(V) surface complexation constants is shown in Table 2. The average absolute error (the average of the absolute differences between the optimized versus jack-knife predicted coefficients) for each soil is also shown. The average and median absolute errors across all 44 soils were 0.377 and 0.286 units, respectively. Ten percent of the soils exhibit errors less than 0.16, 90% of the soils exhibited errors <0.71. Overall, these surface complexation constants appear to be reasonably well estimated (at least for most of the soils). The general good agreement between ordinary predictions and jack-knife estimates suggests that the regression models should have predictive capabilities. The jack-knife MSE estimates for $logK^1_{As}(int)$, $logK^2_{As}(int)$, and $logK^3_{As}(int)$ were found to be 0.181, 0.297, and 0.264, respectively. These estimates are sufficiently close to the ordinary MSE estimates of 0.124, 0.259, and 0.175 produced by the $logK^1_{As}(int)$, $logK^2_{As}(int)$, and $logK^3_{As}(int)$ equations to also suggest predictive ability and parameter stability.

An analysis of the experimentally measured versus model predicted As(V) data was performed to assess both the relative precision and absolute accuracy of the modeling results. The difference between the experimentally determined adsorbed As(V) and the adsorbed As(V) predicted using the jack-knifed regression model surface complexation constants is defined as:

$$\text{Error\_Ad} = \text{Ad}_m - \text{Ad}_e \quad [21]$$

Using this definition, the average mean squared error, AMSE, was calculated from the average of the corresponding uncorrected sum of squares error estimates:

$$\text{AMSE} = \frac{1}{N}\sum_{i=1}^{N}(Error\_Ad)^2 \quad [22]$$

and the corresponding average root mean squared error, ARMSE, to be the square root of this estimate. The ARMSE estimate was used to quantify square root of the total prediction error. That is, the ARMSE represents the square root of both the prediction variance and the average squared bias effects (Myers and Montgomery, 2002), where the variance and bias reflect the relative precision and absolute accuracy between the experimental and jack-knife predicted As(V) adsorption data, respectively. In addition to calculating the ARMSE estimates, a coefficient-of-variation type statistic was also calculated. Specifically, the coefficient-of-imprecision, CIp, was defined to be:

$$\text{CIp} = \frac{100\,\text{ARMSE}}{(\overline{Y}_e + \overline{Y}_m)/2} \quad [23]$$

where the denominator represents the average of the two corresponding soil-specific mean adsorbed As(V) levels. This latter statistic was used to quantify the relative variation in the adsorbed As(V) error distributions with respect to the mean adsorbed As(V) levels.

Three types of statistics are shown in Table 5 for each

Table 5. Relative precision and absolute accuracy statistics for experimentally derived versus constant capacitance model predicted As(V) adsorption levels (n = 44 calibration soils).

Soil series	Depth	Correlation coefficient	ARMSE	CIp
	cm		μmol L^{-1}	
Altamont	0–25	0.850	0.200	19.83
	25–51	0.712	0.337	31.03
Arlington	0–25	0.633	0.389	57.96
	25–51	0.802	0.231	25.93
Avon	0–15	0.761	0.164	30.68
Bonsall	0–25	0.627	0.362	50.07
	25–51	0.735	0.375	29.89
Diablo	0–15	0.765	0.490	63.05
Fallbrook	0–25	0.684	0.132	15.71
	25–51	0.709	0.096	15.40
Fiander	0–15	0.509	0.391	47.83
Haines	20	−0.436	0.352	67.52
Hanford	0–10	0.695	0.269	39.55
Holtville	61–76	0.659	0.433	47.24
Imperial	15–46	0.257	0.298	29.00
Pachappa	0–25	0.554	0.172	21.15
	25–51	0.756	0.102	11.22
Porterville	0–7.6	0.802	0.201	17.95
Ramona	0–25	0.954	0.098	18.88
	25–51	0.521	0.156	19.51
Reagan	Surface	0.193	0.131	17.41
Ryepatch	0–15	0.566	0.265	40.20
Sebree	0–13	0.626	0.150	20.53
Wasco	0–5.1	0.488	0.288	50.07
Wyo		0.448	0.388	39.07
Yolo	0–15	0.660	0.159	14.98
Dennis	A	0.834	0.065	3.95
	B	0.753	0.014	0.73
Dougherty	A	0.425	0.327	42.17
Hanlon	A	0.431	0.347	33.17
Kirkland	A	0.729	0.255	19.12
Luton	A	0.468	0.244	16.96
Mansic	A	0.206	0.555	56.01
	B	−0.785	0.901	146.29
Norge	A	0.588	0.324	27.46
Osage	A	0.223	0.051	2.89
	B	0.831	0.232	13.19
Pond Creek	A	0.764	0.198	17.13
	B	0.763	0.126	8.43
Pratt	A	0.796	0.102	28.34
	B	0.531	0.142	42.21
Richfield	B	0.656	0.477	37.98
Taloka	A	0.763	0.161	14.88
Teller	A	0.628	0.245	25.58

of the 44 calibration soils considered in the study: the Pearson correlation coefficients (which measure just the relative precision, after adjusting out any bias), and the ARMSE and CIp estimates (which quantify both relative precision and absolute accuracy). The adsorption correlation coefficients (Table 5) tend to exhibit considerable variation. These calculated correlation levels range from a high value of 0.954 for the Ramona soil to a low value of 0.206 for the Mansic A horizon. Additionally, two soils (Haines and Mansic B) exhibit negative correlation coefficients, suggesting that the shape of the predicted adsorption envelopes for these two soils is inversely related to the experimental adsorption data. The average correlation level was 0.571, and 50% of the soils exhibit correlations >0.66. The ARMSE estimates expressed on a μmol L^{-1} basis tend to be far less variable. The average ARMSE level across all 44 soils is 0.259; 80% of the soils exhibit values in the range of 0.09 to 0.43. About 95% of the soils exhibit CIp statistics that are <63%, with an average level (across all 44 soils) of 31.3%. Eighty percent of the CIp statistics fall in the range of 11.2 to 56.0%.

Table 6. Parametric and non-parametric tests for prediction bias in experimentally derived versus constant capacitance model predicted As(V) adsorption levels.

		Adsorbed As(V)
	Individual experimental versus model predictions	
	N	527
	USS/N	0.0930
ANOVA	MSE	0.0219
	R-square	0.784
	F-score	40.81
	ndf, ddf	43 483
	Probability > F	<0.0001
Kruskal-Wallis	Chi-square	400.5
	df	43
	Probability > Chi	<0.0001
	Average error analysis (averaged across soils)	
	N	44
	Mean	−0.0053
	Standard deviation	0.2725
	Standard error	0.0411
	t-score	−0.128
	Probability > |t|	0.899
Signed rank	sr-score	−4.0
	Probability > |sr|	0.963

Note that the constant capacitance model was not actually fit to any of the experimental As(V) adsorption data in this prediction analysis. Rather, constant capacitance model predictions were instead generated using the jack-knifed regression model surface complexation constants. Given this fact, it is reasonable to expect that for any specific soil there may be some consistent amount of prediction bias, that is, a consistent shift in location between the experimentally determined versus constant capacitance model predicted As(V) adsorption levels. To test for such effects, we fit a one-way analysis of variance (ANOVA) model to the error distribution, defined as:

$$\text{Error\_Ad}_{ij} = \mu + \alpha_i + \varepsilon_{ij} \quad [24]$$

where i = 1 to 44 represents the 44 specific soils analyzed in this study, and j = 1 to n_i represents the individual observations collected for each soil at the solution pH values (Montgomery, 1997). In this ANOVA model, the F-test on the soil type effects, α, corresponds to a test for detectable within-soil prediction bias. The formal test results for within-soil bias effects are given in the upper portion of Table 6. The ANOVA model for the adsorbed As(V) errors explains about 78% of the total error variation, and the F-score pertaining to the within-soil effect is highly significant ($F = 40.81$, $p < 0.0001$). In addition to the standard (parametric) ANOVA analysis, Eq. [24] was also analyzed using a non-parametric Kruskal–Wallis test (Hollander and Wolfe, 1999). The non-parametric Kruskal–Wallis chi-square tests confirm the parametric results ($\chi^2 = 400.5$, $p < 0.0001$). As expected, there is a significant degree of bias in the adsorbed As(V) errors for specific soils.

To test for between-soil prediction bias, we calculated the mean adsorption errors for each soil and then analyzed the overall average values of these errors using both t tests and non-parametric sign-rank tests. The formal test results for between-soil bias effects are shown in the lower portion of Table 6. The t test and signed rank test results are clearly nonsignificant for the aver-

Table 7. Relative precision and absolute accuracy statistics for experimentally derived versus constant capacitance model predicted As(V) adsorption levels (n = 5 independent prediction soils).

Soil series	Correlation coefficient	ARMSE	CIp
		μmol L^{-1}	
Bernow	0.049	0.185	9.96
Canisteo	0.839	0.816	117.55
Nohili	0.243	0.418	26.02
Summit A	0.397	0.092	5.19
Summit B	−0.124	0.095	5.18

age adsorbed As(V) errors. These results suggest that there is no global bias present in the average constant capacitance model prediction errors across the 44 calibration soils analyzed in this study.

The prediction equations were also used to predict As(V) surface complexation constants for the remaining five soils that had not been used to obtain the general regression model. The constant capacitance model containing these surface complexation constants was used to predict As(V) on the five soils. Since the data from the five soils had not been used to develop the prediction equations, this represents an independent evaluation of their ability to predict As(V) adsorption. Figure 3 indicates the ability of this approach to predict As(V) adsorption on the five soils not used to obtain the prediction equations. Prediction of As(V) adsorption on the Bernow, Summit A, and Summit B soils was good, deviating from the experimental adsorption data by at most 15% for one data point. Prediction of As(V) adsorption on the Nohili soil deviated from the experimental adsorption data by 30% or less. We consider this result to be reasonable since it is a prediction obtained without optimization of any adjustable parameters. Prediction of As(V) adsorption on the Canisteo soil was very poor.

The relative precision and absolute accuracy statistics for the five independently predicted soils are given in Table 7. The Canisteo soil clearly exhibits abnormally large ARMSE and CIp values. The remaining four soils exhibit much more reasonable ARMSE estimates, but significantly degraded correlation values. The CIp statistics for all independently predicted soils, except Canisteo are comparable or smaller than the average for the 44 calibration soils.

Although prediction of As(V) adsorption on one of the soils was poor and on another was only semi-quantitative, for three of the soils the predictions were able to accurately describe As(V) adsorption. The model predictions were obtained independent of any experimental measurement of As(V) adsorption on these soils, using values of easily measured soil chemical parameters. Since our model results are predictions, zero adjustable parameters are used. The present study was performed at a constant initial As(V) concentration. Thus the effect of As(V) loading remains to be investigated. Incorporation of these prediction equations into chemical speciation-transport models should allow simulation of As(V) under aerobic agricultural and environmental conditions. Future research will determine to what extent adequate simulations of As(V) adsorption, release, and transport are possible without the necessity to perform time consuming, detailed studies for each soil.

ACKNOWLEDGMENTS

Gratitude is expressed to Mr. H.S. Forster and Ms. M.M. Mandap for technical assistance, Dr. J.D. Rhoades for providing soil samples, and Mr. S. Nakamura for providing the Nohili soil series classification.

REFERENCES

Arai, Y., D.L. Sparks, and J.A. Davis. 2004. Effects of dissolved carbonate on arsenate adsorption and surface speciation at the hematite–water interface. Environ. Sci. Technol. 38:817–824.

Benjamin, M.M. 2002. Modeling the mass-action expression for bidentate adsorption. Environ. Sci. Technol. 36:307–313.

Chakravarty, S., V. Dureja, G. Bhattacharyya, S. Maity, and S. Bhattacharjee. 2002. Removal of arsenic from groundwater using low cost ferruginous manganese ore. Water Res. 36:625–632.

Cihacek, L.J., and J.M. Bremner. 1979. A simplified ethylene glycol monoethyl ether procedure for assessing soil surface area. Soil Sci. Soc. Am. J. 43:821–822.

Coffin, D.E. 1963. A method for the determination of free iron oxide in soils and clays. Can. J. Soil Sci. 43:7–17.

De Brouwere, K., E. Smolders, and R. Merckx. 2004. Soil properties affecting solid-liquid distribution of As(V) in soils. Eur. J. Soil Sci. 55:165–173.

Dzombak, D.A., and F.M.M. Morel. 1990. Surface complexation modeling: Hydrous ferric oxide, Wiley & Sons, New York.

Fendorf, S., M.J. Eick, P. Grossl, and D.L. Sparks. 1997. Arsenate and chromate retention mechanisms on goethite. 1. Surface structure. Environ. Sci. Technol. 31:315–320.

Gao, Y., and A. Mucci. 2001. Acid base reactions, phosphate and arsenate complexation, and their competitive adsorption at the surface of goethite in 0.7 M NaCl solution. Geochim. Cosmochim. Acta 65:2361–2378.

Gao, Y., and A. Mucci. 2003. Individual and competitive adsorption of phosphate and arsenate on goethite in artificial seawater. Chem. Geol. 199:91–109.

Goldberg, S. 1986. Chemical modeling of arsenate adsorption on aluminum and iron oxide minerals. Soil Sci. Soc. Am. J. 50:1154–1157.

Goldberg, S. 1991. Sensitivity of surface complexation modeling to the surface site density parameter. J. Colloid Interface Sci. 145:1–9.

Goldberg, S. 1992. Use of surface complexation models in soil chemical systems. Adv. Agron. 47:233–329.

Goldberg, S. 2002. Competitive adsorption of arsenate and arsenite on oxides and clay minerals. Soil Sci. Soc. Am. J. 66:413–421.

Goldberg, S., and R.A. Glaubig. 1988. Anion sorption on a calcareous, montmorillonitic soil—Arsenic. Soil Sci. Soc. Am. J. 52:1297–1300.

Goldberg, S., and C.T. Johnston. 2001. Mechanisms of arsenic adsorption on amorphous oxides evaluated using macroscopic measurements, vibrational spectroscopy, and surface complexation modeling. J. Colloid Interface Sci. 234:204–216.

Goldberg, S., S.M. Lesch, and D.L. Suarez. 2000. Predicting boron adsorption by soils using soil chemical parameters in the constant capacitance model. Soil Sci. Soc. Am. J. 64:1356–1363.

Goldberg, S., S.M. Lesch, and D.L. Suarez. 2002. Predicting molybdenum adsorption by soils using soil chemical parameters in the constant capacitance model. Soil Sci. Soc. Am. J. 66:1836–1842.

Goldberg, S., and G. Sposito. 1984. A chemical model of phosphate adsorption by soils. I. Reference oxide minerals. Soil Sci. Soc. Am. J. 48:772–778.

Goldberg, S., D.L. Suarez, N.T. Basta, and S.M. Lesch. 2004. Predicting boron adsorption isotherms by Midwestern soils using the constant capacitance model. Soil Sci. Soc. Am. J. 68:795–801.

Gusstafsson, J.P. 2001. Modelling competitive anion adsorption on oxide minerals and an allophane-containing soil. Eur. J. Soil Sci. 52:639–653.

Herbelin, A.L., and J.C. Westall. 1996. FITEQL: A computer program for determination of chemical equilibrium constants from experimental data. Rep. 96–01, Version 3.2, Dep. of Chemistry, Oregon State Univ., Corvallis.

Hering, J.G., P.-Y. Chen, J.A. Wilkie, M. Elimelich, and S. Liang.

1996. Arsenic removal by ferric chloride. J. Am. Water Works Assoc. 88:155–187.
Hiemstra, T., and W.H. van Riemsdijk. 1999. Surface structural ion adsorption modeling of competitive binding of oxyanions by metal (hydr)oxides. J. Colloid Interface Sci. 210:182–193.
Hollander, M., and D.A. Wolfe. 1999. Nonparametric statistical methods. 2nd ed. John Wiley & Sons, New York.
Hsia, T.H., S.L. Lo, and C.F. Lin. 1992. As(V) adsorption on amorphous iron oxide: Triple layer modeling. Chemosphere 25:1825–1837.
Johnson, R.A., and D.W. Wichern. 1988. Applied multivariate statistical analysis. 2nd ed. Prentice Hall, Englewood Cliffs, NJ.
Khaodhiar, S., M.F. Azizian, K. Osathaphan, and P.O. Nelson. 2000. Copper, chromium, and arsenic adsorption and equilibrium modeling in an iron-oxide-coated sand, background electrolyte system. Water Air Soil Pollut. 119:105–1120.
Livesey, N.T., and P.M. Huang. 1981. Adsorption of arsenate by soils and its relation to selected chemical properties and anions. Soil Sci. 131:88–94.
Lumsdon, D.G., J.C.L. Meeussen, E. Pateson, L.M. Garden, and P. Anderson. 2001. Use of solid phase characterisation and chemical modelling for assessing the behavior of arsenic in contaminated soils. Appl. Geochem. 16:571–581.
Manning, B.A., and S. Goldberg. 1996a. Modeling competitive adsorption of arsenate with phosphate and molybdate on oxide minerals. Soil Sci. Soc. Am. J. 60:121–131.
Manning, B.A., and S. Goldberg. 1996b. Modeling arsenate competitive adsorption on kaolinite, montmorillonite, and illite. Clays Clay Miner. 44:609–623.
Manning, B.A., and D.A. Martens. 1997. Speciation of arsenic(III) and arsenic(V) in sediment extracts by high-performance liquid chromatography—hydride generation atomic absorption spectrophotometry. Environ. Sci. Technol. 31:171–177.
Montgomery, D.C. 1997. Design and analysis of experiments. 5th ed. John Wiley & Sons, New York.
Myers, R.H. 1986. Classical and modern regression with applications. Duxbury Press, Boston, MA.
Myers, R.H., and D.C. Montgomery. 2002. Response surface methodology: Process and product optimization using designed experiments. John Wiley & Sons, New York.
Rhoades, J.D. 1982. Cation exchange capacity. p. 149–157. *In* A.L. Page et al. (ed.) Methods of soil analysis. Part 2. 2nd ed. Agron. Monogr. 9. ASA, Madison, WI.
Sposito, G. 1983. Foundations of surface complexation models of the oxide-aqueous solution interface. J. Colloid Interface Sci. 91:329–340.
Swedlund, P.J., and J.G. Webster. 1999. Adsorption and polymerisation of silicic acid on ferrihydrite, and its effect on arsenic adsorption. Water Res. 33:3413–3422.
Thomas, G.W. 1996. Soil pH and soil acidity. p. 475–490. *In* D.L. Sparks et al. (ed.) Methods of soil analysis. Part 3. SSSA Book Series 5. SSSA, Madison, WI.
Wauchope, R.D. 1975. Fixation of arsenical herbicides, phosphate, and arsenate in alluvial soils. J. Environ. Qual. 4:355–358.
Waychunas, G.A., B.A. Rea, C.C. Fuller, and J.A. Davis. 1993. Surface chemistry of ferrihydrite: Part 1. EXAFS studies of the geometry of coprecipitated and adsorbed arsenate. Geochim. Cosmochim. Acta 57:2251–2269.
Westall, J., and H. Hohl. 1980. A comparison of electrostatic models for the oxide/solution interface. Adv. Colloid Interface Sci. 12: 265–294.
Yang, J.-K., M.O. Barnett, P.M. Jardine, N.T. Basta, and S.W. Casteel. 2002. Adsorption, sequestration, and bioaccessibility of As(V) in soils. Environ. Sci. Technol. 36:4562–4569.